Dynamic mechanical properties of polymer–fluid systems: characterization of poly(2-hydroxyethyl methacrylate) and poly(2-hydroxyethyl methacrylate-*co*-methyl methacrylate) hydrogels

Steven R. Lustig*, James M. Caruthers and Nikolaos A. Peppas†
School of Chemical Engineering, Purdue University, West Lafayette, IN 47907, USA
(Received 26 December 1989; revised 4 January 1991; accepted 4 January 1991)

The complex shear moduli of crosslinked poly(2-hydroxyethyl methacrylate) and poly(2-hydroxyethyl methacrylate-*co*-methyl methacrylate) hydrogels were measured as a function of water content, temperature and frequency using dynamic mechanical spectroscopy. The effect of increasing water content on both the storage and loss moduli is to lower the temperatures at which mechanical transitions occur. There is a significant decrease in the storage moduli and increase in the loss moduli dispersions with increasing water content. These data could be well correlated by a multiple-mechanism, time–temperature superposition procedure. Between 2% and 28% water content in the copolymer sample, the relaxation spectra and shift function characterizing the glassy–rubbery state transition become independent of water content when properly referenced to the observed transition temperature. At lower temperatures where the β transition occurs, the mechanical viscoelastic spectra depend much more strongly on water content although the shift factors collapse to a single curve when referenced to the observed β transition temperature.

(Keywords: hydrogels; dynamic mechanical shear properties; PHEMA; P(HEMA-*co*-MMA); plasticization; time–temperature superposition; viscoelasticity)

INTRODUCTION

A plasticizing diluent significantly affects the mechanical properties of a polymeric solid. A quantitative understanding of plasticization is of considerable importance for polymers used in structural applications exposed to various solvents. The primary objective of this work is to investigate how a strongly plasticizing solvent affects the linear viscoelastic properties. The motivation for this study is recent theoretical work[1,2] that shows the isothermal transport of fluids in polymeric solids is controlled by two macroscopic driving forces: the gradient of the chemical potential and the divergence of the stress tensor. Thus, in order to implement this model an understanding of the effect of solvent concentration on the time-dependent stress is required with particular emphasis on solvent effects in the glassy–rubbery state transition.

The materials of particular interest in this study are synthetic hydrogels of poly(2-hydroxyethyl methacrylate) (PHEMA) and poly(2-hydroxyethyl methacrylate-*co*-methyl methacrylate), [P(HEMA-*co*-MMA], which are used in biomedical applications because of their compatibility with living systems. In general, the surface properties are considered most important in determining whether a particular synthetic hydrogel is biocompatible. The permeability of particular bioactive compounds is also important when they must be transportable through the hydrogel. These considerations are probably sufficient when these materials are to be used as passive diffusion barriers for drug release systems, linings for artificial implants, contact lenses, etc. However, some applications, such as swelling-controlled release systems, exploit the bulk, dynamic properties of hydrogels which can be measured by dynamic mechanical spectroscopy.

Previous investigators have studied the effects of temperature and chemical structure on the dynamic storage and loss moduli at constant shear frequency to understand the origins of viscoelastic mechanical transitions. For vinyl polymers, the α transition is generally attributed to the onset of large scale, cooperative displacements of the methylene chains in the macromolecular networks[3]. The β transition in methacrylates is generally attributed to the onset of the pendant, ester chain mobility[3]. Russell *et al.*[4] investigated the effect of tacticity on the temperature dependent shear modulus for PHEMA using a torsion-pendulum apparatus at 1 Hz. The glassy–rubbery state transition temperature for isotactic PHEMA is ~35°C, some 70°C lower than that for syndiotactic PHEMA. In addition, PHEMA samples with a greater fraction of syndiotactic triads have a more pronounced β transition. The β transition is completely suppressed in isotactic PHEMA. A comparison of the conformational features indicates some interesting differences between isotactic and

* Present address: E.I. du Pont de Nemours & Co., Central Research and Development, Wilmington, DE 19880-0356, USA
† To whom correspondence should be addressed

0032-3861/91/183340-14

syndiotactic chains. Isotactic PHEMA has no intrachain hydrogen bonds linking the ester pendant groups. All the hydroxy groups project out helically, away from the main chain. Syndiotactic PHEMA possesses *trans–gauche–trans* sequences which bring a pair of pendant chains close enough for the terminal hydroxy groups to associate. Rotation of the pendant group about the ester axis would be strongly inhibited in isotactic isomers due to steric hindrance from the α-methyl groups of the neighbouring monomer units. Gillham[5] observed that a relatively strong β transition is exhibited by syndiotactic PMMA while it is all but completely suppressed for isotactic PMMA. Heijboer[6] and Janaćek[7] provided extensive reviews on how systematically substituted chemical groups on amorphous alkyl- and haloalkyl methacrylate polymers affect the glass-to-rubber α-transition, and the sub-glass transition temperature (T_g) β and γ transitions. Janaćek[7], and Janaćek and Kolařik[8] additionally considered the effects of diluents. In general, polar groups, comonomers and diluents mostly affect the β and γ transitions in a similar manner as they affect the α transition. Polar groups in the pendant chains and steric hindrance increase the transition temperatures. Increasing diluent composition causes a decrease in the mechanical transition temperatures. While these studies indicate important, qualitative trends, the complete time- or frequency-dependent material response cannot be inferred from their data. In this study we will report on the frequency-dependent viscoelastic properties as a function of temperature and concentration in order to construct the complete linear viscoelastic master curve.

EXPERIMENTAL

Sample synthesis and preparation

The polymers used in this study were synthesized by addition polymerization of 2-hydroxyethyl methacrylate (HEMA), methyl methacrylate (MMA), ethylene glycol dimethacrylate (EGDMA) monomers and 2,2′-azobis(2-methyl propionitrile) (AIBN) initiator. It is difficult to prepare completely pure HEMA since hydrolysis and transesterification reactions produce small amounts of methacrylic acid and EGDMA. Low-acid grade HEMA monomer (liquid, 98%) was supplied by Polysciences (Warrington, PA, USA). The MMA (liquid, 99%), EGDMA (liquid, 99%) and AIBN (crystalline, >99%) were obtained from Aldrich (Milwaukee, WI, USA).

Three monomer mixtures were prepared by weighing the desired amount of each component according to the compositions in *Table 1*. Each mixture was then sonicated to dissolve the AIBN and degassed by freezing–evacuation steps repeated three times. After degassing, the mixture was introduced into a mould. Two brass plates ($\sim 25 \times 18 \times 0.2$ cm) formed a cavity for the liquid monomer feed. A protective overlay supplied by Cole-Parmer (Chicago, IL, USA) was adhered to the inner face of each brass plate. This had a Teflon® surface adhered to the inside mould cavity. The mould cavity was laterally defined with an FEP Freeway Teflon®-coated, silicone O-ring. Brass spacers between the plates were just thick enough to compress the O-ring sufficiently to form a seal. The inside mould cavity had nominal dimensions $\sim 19 \times 11 \times 0.3$ cm. The outer brass frame pieces provided structural rigidity to the mould as well as open area for heat transfer to the ~ 0.2 cm thick brass plates. This assembly was found to be quite reliable in averting leakage from the mould cavity and preventing adhesion to the newly formed polymer. No mould-release agents were required.

The polymerization was carried out with a variable temperature history to promote complete conversion while avoiding a thermally uncontrolled reaction. First, the mould was placed in a temperature-controlled water bath at 50°C for 48 h. Here the monomers polymerized to a gel state. This step provided sufficient thermal, homolytic dissociation of the AIBN initiator yet avoided autoaccelerated, thermal run-away. Second, the mould was immediately placed in a temperature-controlled water bath at 80°C for 24 h. The polymerization mixture vitrified during this step. Last, the mould was placed in a convection oven at 110°C for 24 h to anneal the polymer above its final T_g. The oven was then turned-off and allowed to cool to room temperature over a period of ~ 8 h. This ensured that the polymerization was complete, shrinkage stresses were relaxed and that the thermal histories for all specimens were identical and reproducible through this point. The moulded sheets were stored in a desiccator at room temperature.

Determination of structural tacticity

Finely ground samples of the PHEMA, P(HEMA-*co*-MMA) and PMMA polymers were dissolved in pyridine-d_5, pyridine-d_5 and chloroform-d, respectively, and sealed in nuclear magnetic resonance (n.m.r) tubes. ^{13}C-n.m.r spectra were collected on an n.m.r. spectrometer (model XL-200A, Varian Park Ridge, IL, USA) at 50 MHz. No isotactic triads could be detected on any of the polymers. Syndiotactic and heterotactic triads pertaining to the α-methyl groups on the methacrylate repeating units were detected. The relative contents of syndiotactic triads in the PHEMA, P(HEMA-*co*-MMA) and PMMA polymers were calculated as 44, 70 and $62 \pm 10\%$, respectively.

Table 1 Feed compositions for polymers[a]

	PHEMA		P(HEMA-*co*-MMA)		PMMA	
Monomer	Mole fraction	Weight fraction	Mole fraction	Weight fraction	Mole fraction	Weight fraction
HEMA	0.9985	0.9976	0.6990	0.7501	–	–
MMA	–	–	0.2996	0.2473	0.9985	0.9969
EGDMA	0.0010	0.0019	0.0010	0.0020	0.0010	0.0024

[a] In all cases the initiator AIBN content was 0.05 mol%

Linear viscoelastic shear modulus

Samples were cut from the moulded sheets into strips of nominal dimensions $\sim 6 \times 1 \times 0.3$ cm using a low-speed, glass cutter (Buehler Ltd, Lake Bluff, IL, USA). The strips had square edges and uniformly flat faces. Samples to contain water were first weighed dry and then placed in separate containers with deionized water. These containers were kept in a temperature-controlled water bath at 80°C and periodically reweighed. Once a sample had imbibed up to 110% of its predesignated water content, it was kept uncovered on an analytical balance to dry to its final weight. Although the initial water loss was quite rapid, the hydrogel developed a dry skin which increasingly retarded the evaporation. Once the desired weight was obtained, each sample was quickly coated with highly viscous, petroleum gel and stored in a separate container of paraffin oil. These samples were then stored at room temperature for at least 4 days. Previous integral sorption experiments indicated 4 days was a sufficient period to allow the water to attain a uniform concentration distribution. In addition, it had also been determined that these samples could be stored in this manner for 2 weeks before any weight loss could be detected on an analytical balance.

The experiments described here were performed on a dynamic mechanical spectrometer (Rheometrics, model RMS-800, Piscataway, NJ, USA) with a 2 kg normal and torsional force load cell. The applied strain was accurate to within 0.1% of the selected frequency and 0.025% of the selected magnitude. The load transducer was checked to ensure its response did not deviate from previous calibration. For experimental temperatures from room temperature to −150°C a liquid nitrogen evaporator was used to provide cooling. Dry air was used for experiments above room temperature. The sample environmental chamber temperature could be controlled to within ±0.5°C from −150 to −20°C, ±1.5°C from −20 to 15°C, and ±0.5°C from 15 to 300°C.

Samples containing water were installed in the rheometer after being quenched to −150°C using the rheometer's environmental chamber. During installation the sample was requenched if the temperature rose to −30°C. A uniform layer, ~1 mm thick, of either petroleum gel or silicone vacuum grease was applied to the outside of each frozen sample to prevent water loss. The petroleum gel was able to withstand temperatures up to 45°C and the silicone grease was effective up to 80°C. Above these limits, water loss was apparent during the rheological measurements as the moduli began to increase with temperature. Tests on dry samples both with and without a coating indicated that the coating did not affect the viscoelastic measurements.

A series of tests were run to verify that the stress–strain response was in the linear region. Initially, it had been determined that the shear strain should be 0.1% in the glassy state and varied from 0.2 to 0.5% in the glass transition and rubbery state. This ensured that the deformation was linear and the torque was high enough to be detectable accurately by the transducer. The temperature- and frequency-dependent, dynamic shear modulus $G^*(T, \omega)$ was measured by scanning the frequency at temperatures from −150°C to well above T_g. At each temperature, the instrument allowed the sample to equilibrate thermally for 2 min and measured the shear modulus at 16 frequencies evenly spaced logarithmically between 0.1 and 100 rad s^{-1}. To prevent the sample from buckling due to thermal expansion, slight tension was applied at all temperatures. The maximum test temperatures were limited by water loss which occurred when the coating did not adhere to the specimen. This was especially problematic for the samples containing lower water contents since their glassy–rubbery state transition occurs at higher temperatures.

RESULTS

Effect of copolymerization

The storage (G') and loss (G'') shear moduli for dry PHEMA, P(HEMA-*co*-MMA) and PMMA at 1 Hz are illustrated in *Figure 1* between −100°C and 200°C. At the highest temperatures, the three materials exhibit rubbery plateaus at nearly the same values of the storage modulus indicating that the materials have been effectively crosslinked to essentially the same degree. The α, β and γ transitions are designated as relative maxima in the loss modulus data occurring at progressively lower temperatures. All polymers show α and β transitions between these temperatures. The α transitions in the PHEMA, P(HEMA-*co*-MMA) and PMMA data correspond to the glassy–rubbery state transitions and occur at 103, 88 and 117 ± 3°C, respectively, at a frequency of 1 rad s^{-1}. A broad β transition as seen by the loss modulus data occurs at 9 ± 3°C for PMMA and 16 ± 3°C for the copolymer. The broad shoulder in the α transition below T_g indicates a β transition in the PHEMA. The beginning of a γ transition could be observed only for PHEMA and the copolymer. It is interesting that the copolymer exhibits both β and γ transitions while each homopolymer exhibits only one prominent transition below the glass transition, possibly indicating that the comonomer groups have an additive effect on the macroscopic response.

Effect of water content

The effects of water content on the shear moduli for PHEMA and P(HEMA-*co*-MMA) are illustrated in *Figures 2* and *3*, respectively. The effect of increasing water content on both G' and G'' for both polymers is to lower the temperature, T_α, at which the α transition occurs. There is also a decrease in G' magnitude with increasing water content. The β transition maximum for

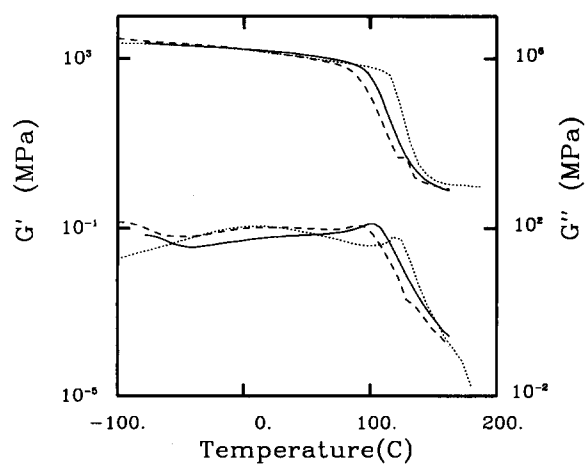

Figure 1 Storage moduli (upper curves) and loss moduli (lower curves) as a function of temperature at 1 Hz for dry PHEMA (——), P(HEMA-*co*-MMA) (– – –) and PMMA (-----)

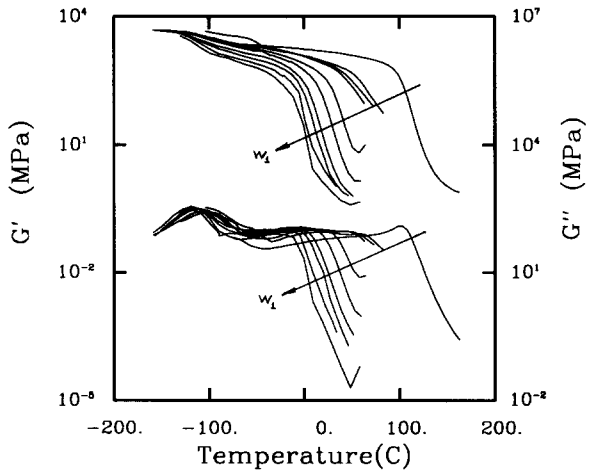

Figure 2 Storage moduli (upper curves) and loss moduli (lower curves) as a function of temperature at 1 Hz for PHEMA hydrogels containing different water contents. In the direction indicated by the arrows, curves correspond to the following water weight fractions: 0.000, 0.040, 0.049, 0.065, 0.085, 0.121, 0.162, 0.199, 0.237 and 0.276

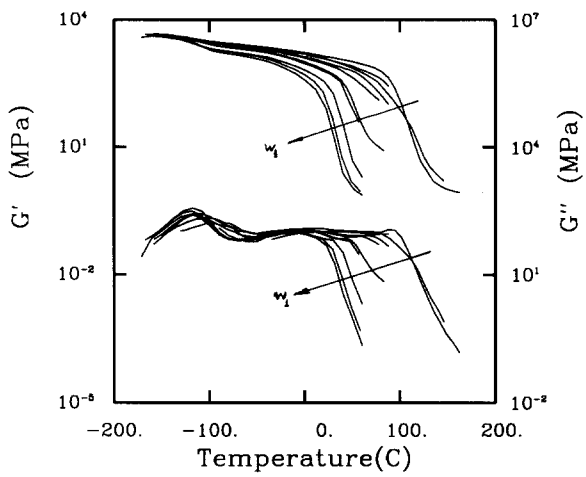

Figure 3 Storage moduli (upper curves) and loss moduli (lower curves) as a function of temperature at 1 Hz for P(HEMA-*co*-MMA) hydrogels containing different water contents. In the direction indicated by the arrows, curves correspond to the following water weight fractions: 0.000, 0.020, 0.032, 0.040, 0.050, 0.100, 0.111, 0.144, 0.177 and 0.204

both polymers becomes more pronounced in magnitude although the transition temperature, T_β, does not decrease as rapidly with increasing water content as does T_α. The γ transition temperature, T_γ, also decreases slightly with increasing water content. Not only do the G'' maxima increase with water content, but there is a more prominent change in G' pertaining to the γ transition. For both the PHEMA–water and P(HEMA-*co*-MMA)–water systems, the loss modulus α transition maximum coalesces into the β transition maximum at the higher water contents. This phenomenon is somewhat frequency-dependent as illustrated in *Figures 4* and *5*. All transition temperatures are observed to decrease with increasing water content and increase with frequency. Still, T_α decreases most rapidly with water content and T_β increases most rapidly with frequency.

TIME–TEMPERATURE SUPERPOSITION

The complete viscoelastic response is traditionally constructed from isotherms over a limited range of times/frequencies by time–temperature superposition[9] (TTS), which assumes the effect of temperature on time-dependent material properties is equivalent to a change in the time scale. Specifically,

$$G'[\omega, T] = G'[\omega a_T(T), T_R] \quad (1)$$

$$G''[\omega, T] = G''[\omega a_T(T), T_R] \quad (2)$$

where the temperature-dependent shift function a_T is unity at an arbitrarily chosen reference temperature, T_R. When isothermal moduli of a thermorheologically simple material are plotted as a function of frequency on a logarithmic abscissa, they can be superposed by a purely horizontal shift along the logarithmic frequency abscissa. The resulting complete response for either G' or G'' is known as a master curve.

Time–temperature superposition was applied to the isotherms of dry PHEMA from −80°C to 162°C as shown in *Figure 6* with the associated $\log a_T$ shift factor in *Figure 7*. Good superposition of the isotherms was obtained above T_g and partial superposition of the isotherms could be achieved in the β transition region; however, the isotherms exhibit systematic lack of superposition in the regions between the α and β transitions and the β and γ transitions. Alternative shifting procedures cannot make any significant improvements in the composite master curve. Specifically, the G' isotherms below T_g could be shifted to achieve good superposition, since the isotherms are essentially linear functions of $\log \omega$. But, this would effect an even greater loss of superposition in the G'' isotherms, and the time–temperature superposition requires that the same $\log a_T$ shift be applied to both the G' and G'' isotherms. Similar problems in applying time–temperature superposition also occurred with the dry P(HEMA-*co*-MMA) and PMMA polymers, with good superposition above T_g and in the β transition region with gross lack of superposition in the regions between the various transitions. Above T_g where superposition was achieved, the $\log a_T$ shift could be described by the Williams–Landel–Ferry (WLF) equation[9] as illustrated in *Figure 7*. The WLF constants for the three materials are given in *Table 2*.

Although traditional TTS cannot be used for PHEMA, P(HEMA-*co*-MMA) and PMMA the isotherms were superposable near the individual transitions. The α and β transitions could be individually thermorheologically simple, each described empirically as a separate relaxation mechanism. A multiple mechanism time–temperature superposition (MMTTS) procedure has been developed[10,11] which acknowledges individual

Table 2 Empirical fit of the WLF equation to the PHEMA, P(HEMA-*co*-MMA) and PMMA shift functions in the glass transition region[a]

	T_R (°C)	C_1	C_2 (°C)
PHEMA	95.2	88.0	117.0
P(HEMA-*co*-MMA)	17.4	13.8	11.6
PMMA	100.0	75.0	38.9

[a] Use of the WLF equation was made for $T > T_R$:

$$\log[a_T] = \frac{-C_1[T - T_R]}{C_2 + T - T_R}$$

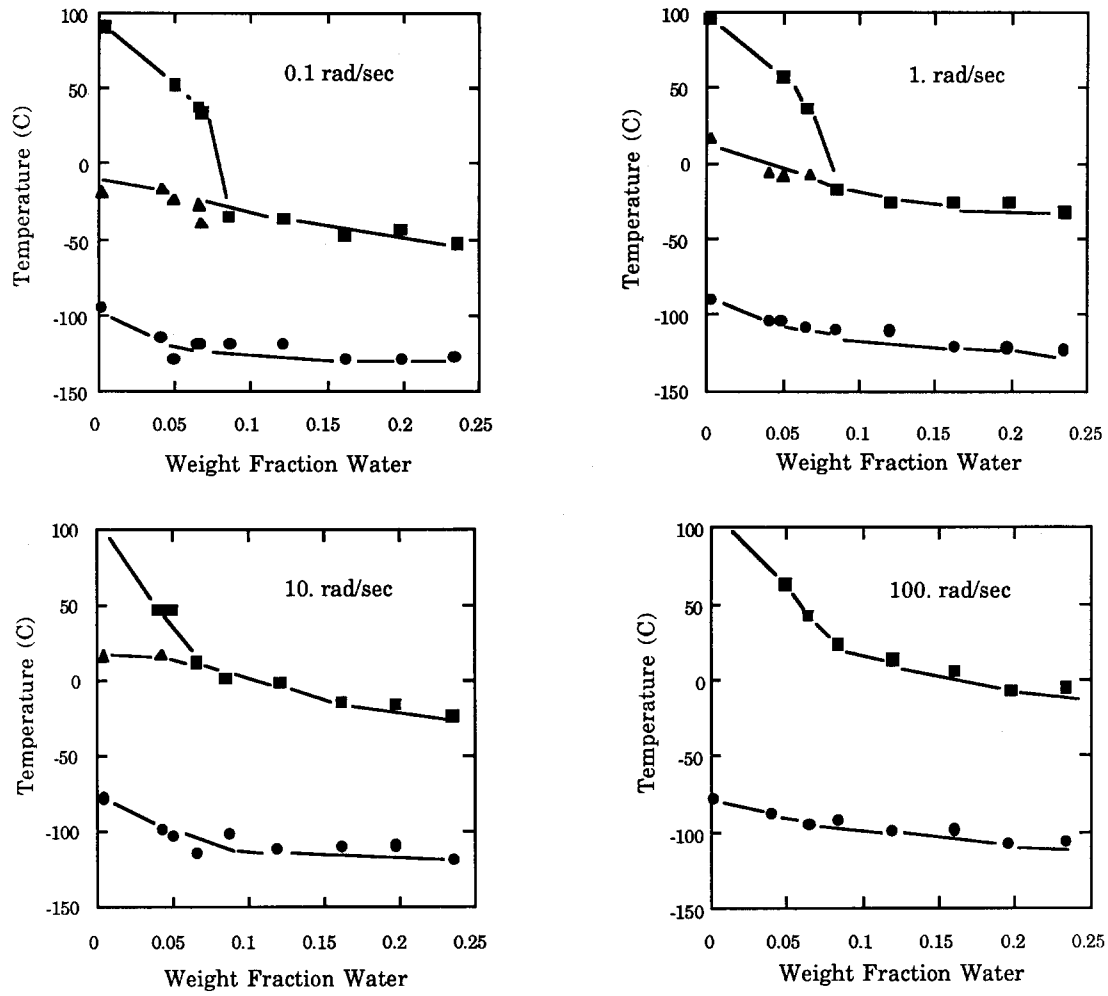

Figure 4 Transition temperatures, T_α (■), T_β (▲), T_γ (●), for PHEMA hydrogels as a function of water weight fraction, as determined from the maxima in the shear loss modulus at 0.1, 1.0, 10.0 and 100.0 rad s^{-1}

contributions to transition mechanisms. This MMTTS analysis assumes that:

1. The α transition response is thermorheologically simple and its temperature dependence can be described by a shift function a_T^α;
2. The β transition response is thermorheologically simple and its temperature dependence can be described by a shift function a_T^β;
3. The observed mechanical response is the additive response due to the α and β mechanisms;
4. The storage modulus can contain a purely elastic, frequency-independent contribution, G_E.

Consequently, the storage and loss moduli are given by:

$$G'[\omega, T] = G_E(T) + G'_\alpha[\omega a_T^\alpha(T), T_R^\alpha] + G'_\beta[\omega a_T^\beta(T), T_R^\beta] \quad (3)$$

$$G''[\omega, T] = G''_\alpha[\omega a_T^\alpha(T), T_R^\alpha] + G''_\beta[\omega a_T^\beta(T), T_R^\beta] \quad (4)$$

Here, a_T^α and a_T^β are both unity at their respective reference temperatures. The frequency-dependent functions are represented by:

$$G'_\alpha(\omega, T) = \sum_{\text{all } i} H_i^\alpha(T_R^\alpha) \frac{(\omega a_T^\alpha \tau_i^\alpha)^2}{1 + (\omega a_T^\alpha \tau_i^\alpha)^2} \quad (5)$$

$$G''_\alpha(\omega, T) = \sum_{\text{all } i} H_i^\alpha(T_R^\alpha) \frac{\omega a_T^\alpha \tau_i^\alpha}{1 + (\omega a_T^\alpha \tau_i^\alpha)^2} \quad (6)$$

For materials which exhibit two relaxation mechanisms, the experimental observed storage and loss moduli are determined by combining equations (3)–(6). The final correlations[10,11] are given below in terms of discrete viscoelastic spectra:

$$G'[\omega, T] = G_E(T) + \sum_{\text{all } i} H_i^\alpha(\tau_i^\alpha, T_R^\alpha) \frac{(\omega a_T^\alpha \tau_i^\alpha)^2}{1 + (\omega a_T^\alpha \tau_i^\alpha)^2} + \sum_{\text{all } j} H_j^\beta(\tau_j^\beta, T_R^\beta) \frac{(\omega a_T^\beta \tau_j^\beta)^2}{1 + (\omega a_T^\beta \tau_j^\beta)^2} \quad (7)$$

$$G''[\omega, T] = \sum_{\text{all } i} H_i^\alpha(\tau_i^\alpha, T_R^\alpha) \frac{\omega a_T^\alpha \tau_i^\alpha}{1 + (\omega a_T^\alpha \tau_i^\alpha)^2} + \sum_{\text{all } j} H_j^\beta(\tau_j^\beta, T_R^\beta) \frac{\omega a_T^\beta \tau_j^\beta}{1 + (\omega a_T^\beta \tau_j^\beta)^2} \quad (8)$$

It is a rather straightforward procedure to extend this MMTTS analysis to more than two relaxational mechanisms. If the data can be described by MMTTS, it will be possible to analyse how the viscoelastic properties depend upon the composition of the various hydrogels. The details of the MMTTS procedures are described via an example using the dry PHEMA data.

Examining equations (7) and (8) indicates that the viscoelastic spectra should be determined from the

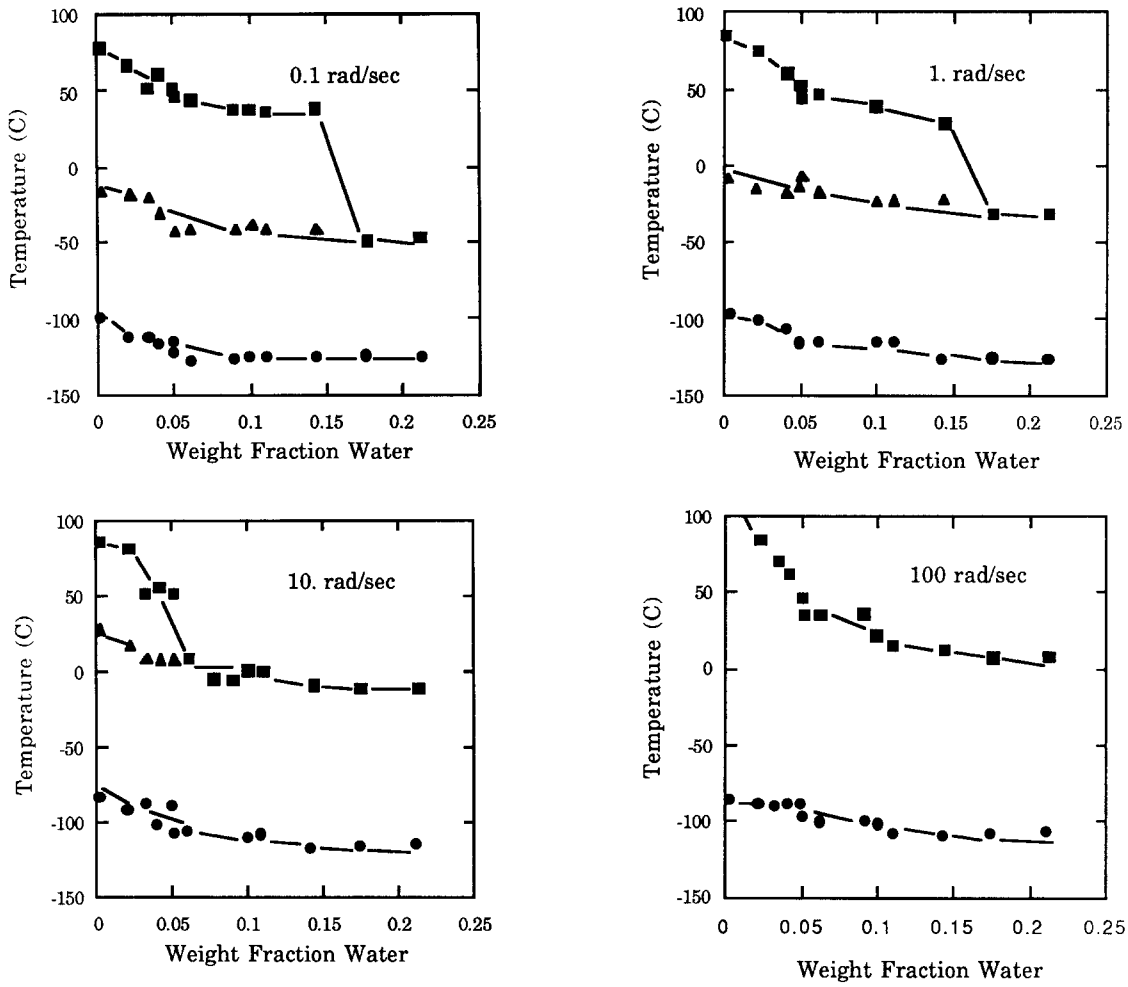

Figure 5 Transition temperatures, T_α (■), T_β (▲), T_γ (●), for P(HEMA-*co*-MMA) hydrogels as a function of water weight fraction, as determined from maxima in the shear loss modulus at 0.1, 1.0, 10.0 and 100.0 rad s^{-1}

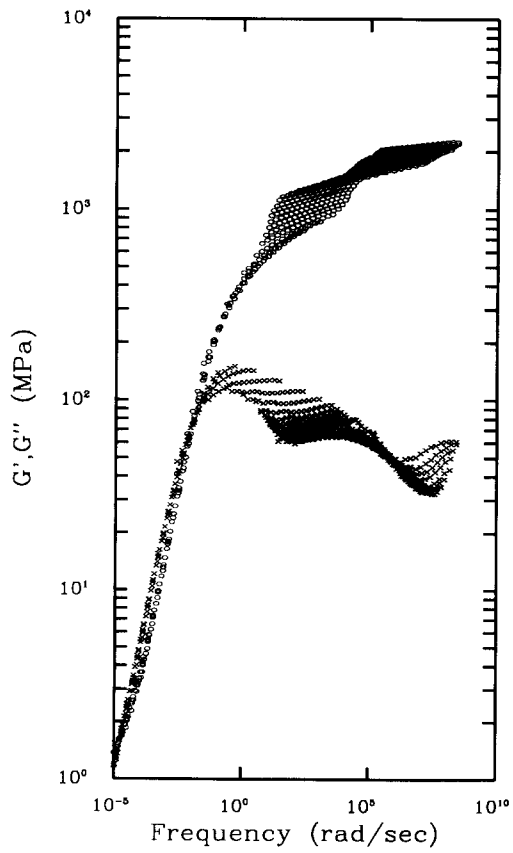

Figure 6 Traditional time–temperature superposition for the storage modulus (○) and loss modulus (×) of dry PHEMA isotherms between −80°C and 160°C

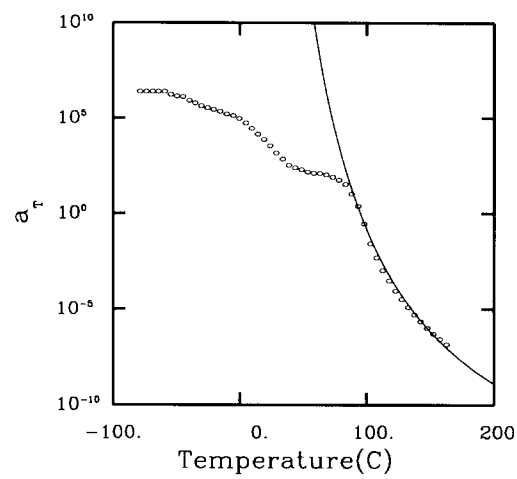

Figure 7 The temperature-dependent shift function used for time–temperature superposition in *Figure 6* (○) and the WLF fit to the glass transition region (——). The WLF parameters are given in *Table 2*

dynamic loss modulus data, since the storage modulus contains a temperature-dependent elastic contribution. First, the log $G''(\omega, T)$ isotherms were plotted separately as a function of log ω. Next, log $G''_\alpha(\omega, T_R^\alpha)$ and log $G''_\beta(\omega, T_R^\beta)$ master curves and the associated log a_T^α and log a_T^β were

constructed by horizontally shifting the individual isotherms so that maximum superposition was obtained, respectively, in the α and β transition regions. The chosen T_R^α (or T_R^β) were the transition temperatures T_α (or T_β) at the maxima in the G'' data at 1 rad s^{-1}. The H_i^α and H_j^β spectra were computed from the $G''(\omega, T)$ data using one of two methods. Curliss[10] provides a regularized quadratic programming algorithm (RQP) to determine simultaneously the H_i^α and H_j^β spectra. The RQP algorithm worked well for G'' data in which the values of the α and β maxima were large relative to the values in the thermorheologically complex regions. In situations where the α and β transitions are not well separated, the RQP algorithm failed to compute spectra which would reproduce the data. In these cases, previous spectra were adjusted interactively by trial and error on a computer workstation until the new spectra were able to fit the experimental data.

The loss modulus master curves for the α and β transitions of PHEMA are shown in *Figure 8* as well as the fits computed from their respective viscoelastic spectra. The thermorheologically complex regions in between the two pronounced transitions are not included in these isotherms; however, the beginning of this

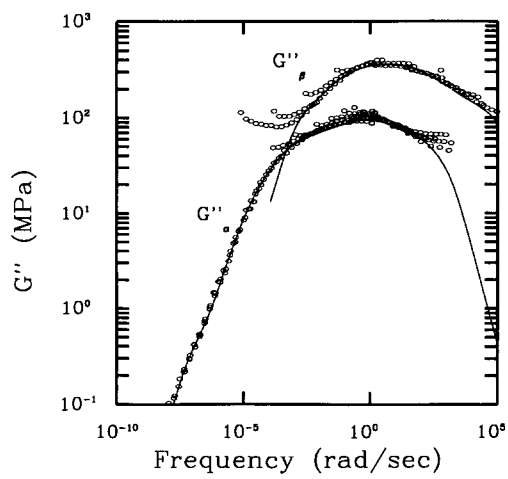

Figure 8 Loss modulus master curves for the α and β transitions of dry PHEMA (○) as well as the empirical fits (——) computed from their respective viscoelastic spectra. The thermorheologically complex regions in between the two pronounced transitions are neglected

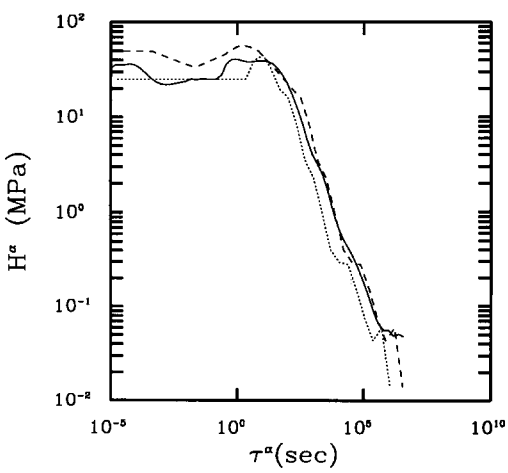

Figure 9 Viscoelastic spectra for the α mechanism of dry PHEMA (——), P(HEMA-*co*-MMA) (– –) and PMMA (-----)

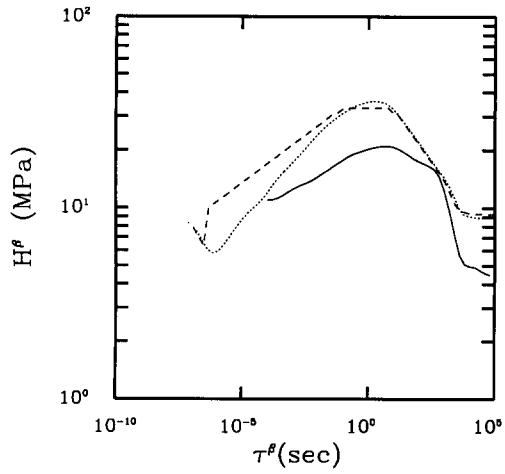

Figure 10 Viscoelastic spectra for the β mechanism of dry PHEMA (——), P(HEMA-*co*-MMA) (– –) and PMMA (-----)

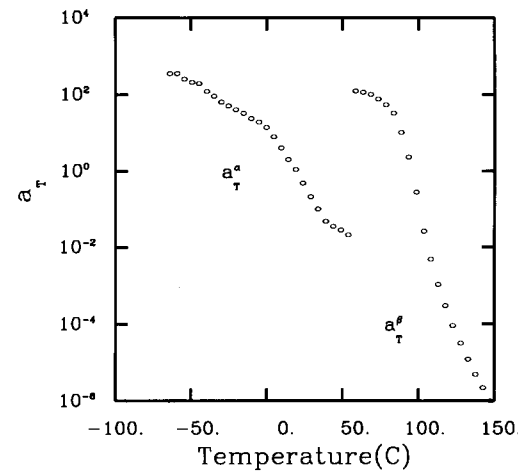

Figure 11 Independent α and β transition shift functions, a_T^α and a_T^β, for dry PHEMA as functions of temperature. The reference temperatures are 95.2 and 19.3°C, respectively

region between the α and β mechanisms is observed in the lack of superposition at high frequencies for the α mechanism and low frequencies for the β mechanism. The relaxation spectra for PHEMA H_i^α and H_j^β are shown in *Figures 9* and *10*. In all plots of relaxation spectra $H_i^\alpha(\tau_i^\alpha)$ and $H_j^\beta(\tau_j^\beta)$, there are five evenly spaced, discrete relaxation times per decade. The temperature-dependent and the $\log a_T^\alpha$ and $\log a_T^\beta$ shift functions are given in *Figure 11*. The temperature-dependent elastic modulus, G_E, was computed by subtracting the now known viscoelastic contribution in equation (7) from the isochronal temperature-dependent storage modulus data at $\omega_1 = 1$ rad s^{-1}. Specifically,

$$G_E[T] = G'(\omega_1, T) - \sum_{\text{all } i} H_i^\alpha(\tau_i^\alpha, T_R^\alpha) \frac{(a_T^\alpha \tau_i^\alpha \omega_1)^2}{1 + (a_T^\alpha \tau_i^\alpha \omega_1)^2} - \sum_{\text{all } j} H_j^\beta(\tau_j^\beta, T_R^\beta) \frac{(a_T^\beta \tau_j^\beta \omega_1)^2}{1 + (a_T^\beta \tau_j^\beta \omega_1)^2} \quad (9)$$

G_E was observed to be independent of temperature over the experimentally accessible frequency range as shown in *Figure 12* for PHEMA. Random variations in the G' and G'' data ultimately limit the accuracy of the measurements and can produce commensurate uncertainty in the

viscoelastic spectra, shift functions and elastic modulus. Hence fluctuations can appear in the computed values for these material functions. Additional details on the calculation procedure are given elsewhere[2,10].

After the spectra and shift functions were obtained for both relaxation mechanisms, equations (7) and (8) were used to calculate the storage and loss moduli at the same frequencies and temperatures at which the original data had been measured. The comparisons for dry PHEMA are shown in detail in *Figures 13–20*. *Figures 13–16* illustrate comparisons between the MMTTS fitting equations and the G' data for dry PHEMA, and *Figures 17–20* illustrate the analogous comparisons for the G'' data. Since only the α and β mechanisms have been characterized, the comparisons are truncated at temperatures below the β transition. *Figure 21* illustrates comparisons between the MMTTS fitting equations and the isochronal storage and loss modulus data at 1 Hz as a function of temperature for dry PHEMA, P(HEMA-*co*-MMA) and PMMA, respectively. Both the storage and loss modulus data can be reproduced satisfactorily.

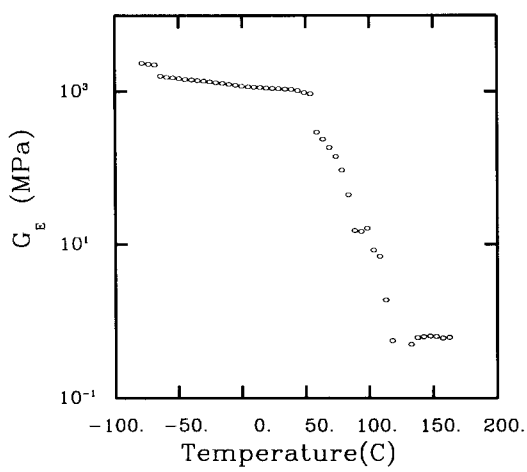

Figure 12 Temperature-dependent, elastic contribution to the dynamic shear modulus for dry PHEMA

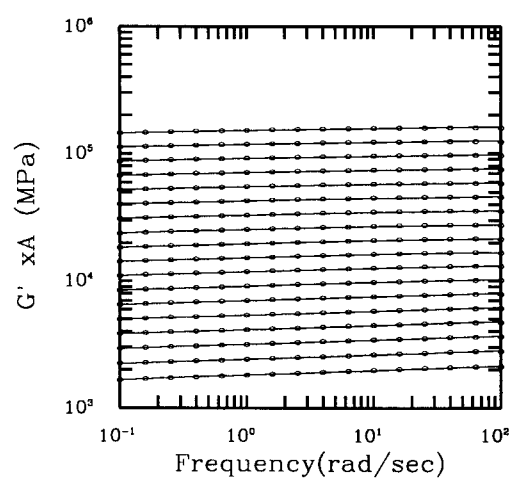

Figure 13 Storage modulus isotherms for dry PHEMA between −35.2°C and 48.6°C showing experimental data (○) and the calculated MMTTS fit (——). From top to bottom, the curves correspond to temperatures (vertical shifts, A) of (°C): −35.2 (1.9), −30.4 (1.8), −25.6 (1.7), −20.7 (1.6), −15.7 (1.5), −10.6 (1.4), −5.5 (1.3), −0.5 (1.2), 4.4 (1.1), 9.2 (1.0), 13.9 (0.9), 18.7 (0.8), 23.6 (0.7), 28.6 (0.6), 33.5 (0.5), 38.5 (0.4), 43.4 (0.3), 48.6 (0.2)

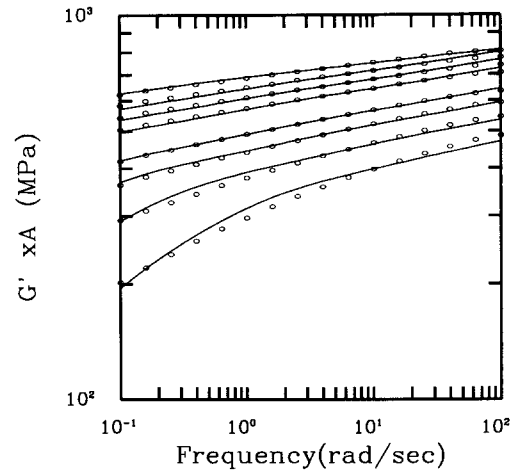

Figure 14 Storage modulus isotherms for dry PHEMA between 53.5°C and 93.3°C showing experimental data (○) and the calculated MMTTS fit (——). From top to bottom, the curves correspond to temperatures (vertical shifts, A) of (°C): 53.5 (−0.2), 58.4 (−0.2), 63.3 (−0.2), 68.3 (−0.2), 78.3 (−0.2), 83.3 (−0.2), 88.3 (−0.2), 93.3 (−0.2)

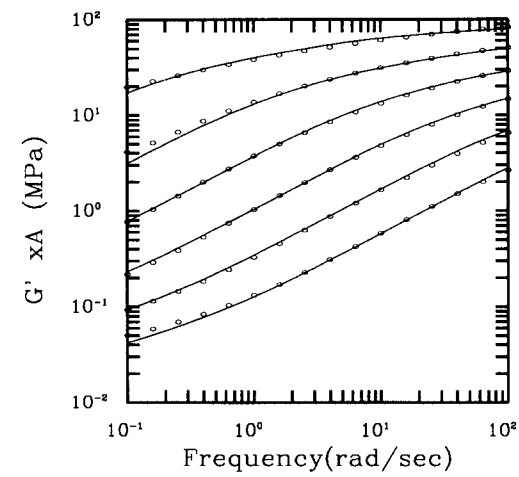

Figure 15 Storage modulus isotherms for dry PHEMA between 98.2°C and 122.6°C showing experimental data (○) and the calculated MMTTS fit (——). From top to bottom, the curves correspond to temperatures (vertical shifts, A) of (°C): 98.2 (−0.9), 103.1 (−1.0), 107.9 (−1.1), 112.8 (−1.2), 117.7 (−1.3), 122.6 (−1.4)

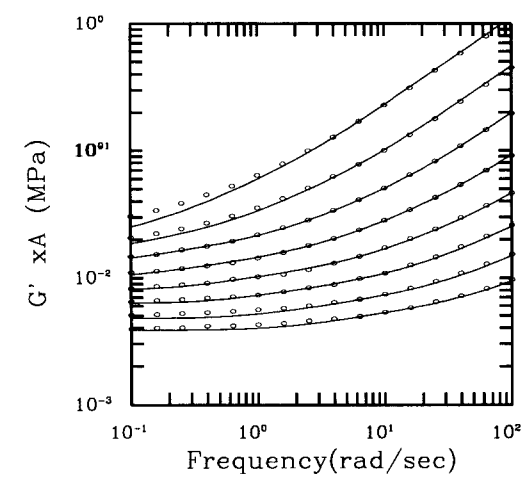

Figure 16 Storage modulus isotherms for dry PHEMA between 127.6°C and 162.3°C showing experimental data (○) and the calculated MMTTS fit (——). From top to bottom, the curves correspond to temperatures (vertical shifts, A) of (°C): 127.6 (−1.5), 132.5 (−1.6), 137.4 (−1.7), 142.4 (−1.8), 147.4 (−1.9), 152.3 (−2.0), 157.3 (−2.1), 162.3 (−2.2)

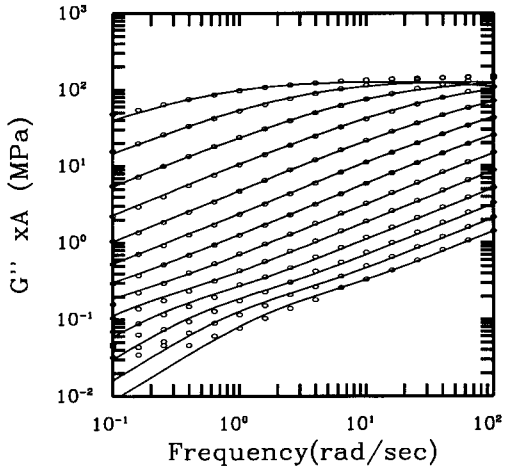

Figure 17 Loss modulus isotherms for dry PHEMA between 103.1°C and 162.3°C showing experimental data (○) and the calculated MMTTS fit (——). From top to bottom, the curves correspond to temperatures (vertical shifts, A) of (°C): 103.1 (0.0), 107.9 (0.0), 112.8 (0.0), 117.7 (0.0), 122.6 (0.0), 127.6 (0.0), 132.5 (0.0), 137.4 (0.0), 142.4 (0.0), 147.4 (0.0), 152.3 (0.0), 157.3 (0.0), 162.3 (0.0)

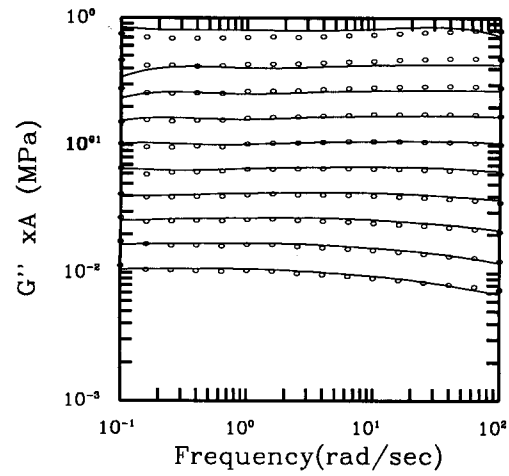

Figure 19 Loss modulus isotherms for dry PHEMA between 13.9°C and 58.4°C showing experimental data (○) and the calculated MMTTS fit (——). From top to bottom, the curves correspond to temperatures (vertical shifts, A) of (°C): 58.4 (−2.0), 53.5 (−2.2), 48.6 (−2.4), 43.5 (−2.6), 38.5 (−2.8), 33.5 (−3.0), 28.6 (−3.2), 23.6 (−3.4), 18.7 (−3.6), 13.9 (−3.8)

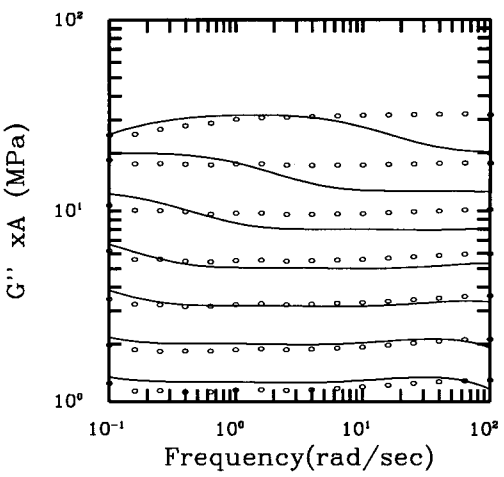

Figure 18 Loss modulus isotherms for dry PHEMA between 63.3°C and 98.2°C showing experimental data (○) and the calculated MMTTS fit (——). From top to bottom, the curves correspond to temperatures (vertical shifts, A) of (°C): 98.2 (−0.6), 93.3 (−0.8), 88.3 (−1.0), 83.3 (−1.2), 78.3 (−1.4), 68.3 (−1.6), 63.3 (−1.8)

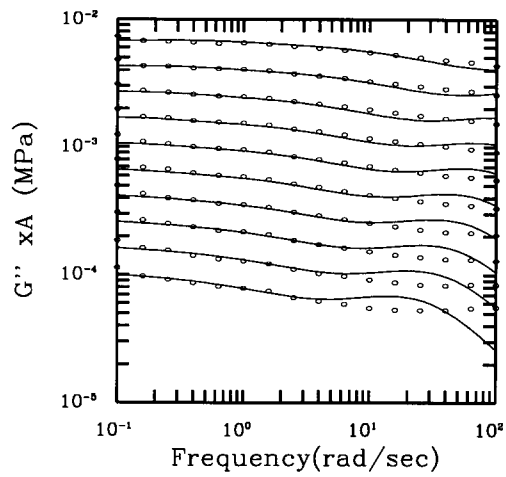

Figure 20 Loss modulus isotherms for dry PHEMA between −35.2°C and 9.2°C showing experimental data (○) and the calculated MMTTS fit (——). From top to bottom, the curves correspond to temperatures (vertical shifts, A) of (°C): 9.2 (−4.0), 4.4 (−4.2), −0.5 (−4.4), −5.5 (−4.6), −10.6 (−4.8), −15.7 (−5.0), −20.7 (−5.2), −25.6 (−5.4), −30.4 (−5.6), −35.2 (−5.8)

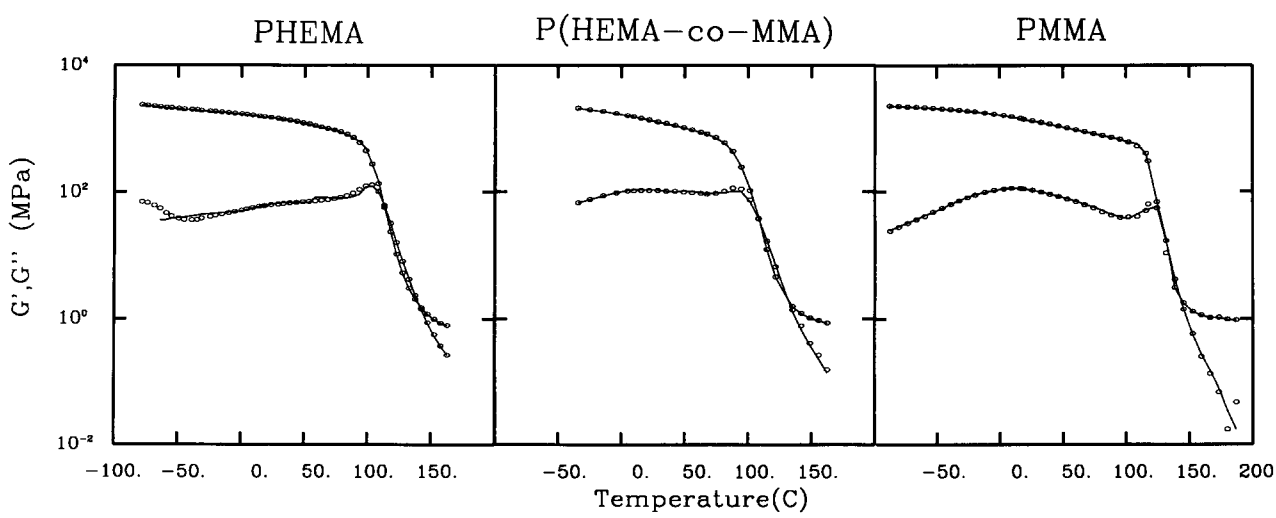

Figure 21 Isochronal storage moduli (upper curves) and loss moduli (lower curves) for dry PHEMA, P(HEMA-*co*-MMA) and PMMA at 1 Hz. Experimental measurements (○) and the calculated MMTTS fit (——) are compared for the α and β transitions only

It is worth noting that since the P(HEMA-*co*-MMA) and PMMA data contain more distinct separation between the α and β relaxations than those for PHEMA, the MMTTS fit to the P(HEMA-*co*-MMA) and PMMA data is always better than that for PHEMA.

VISCOELASTIC PROPERTIES

The viscoelastic properties obtained from the MMTTS analysis are presented here. First the dynamic viscoelastic properties of dry PHEMA, P(HEMA-*co*-MMA) and PMMA will be analysed, and subsequently the effect of water on the viscoelastic properties of PHEMA and P(HEMA-*co*-MMA) will be presented.

Effect of copolymerization

Since only three different polymers are considered, a limited study on the effects of copolymerization is possible. The $\log a_T^\alpha$ and $\log a_T^\beta$ shift functions for PHEMA, P(HEMA-*co*-MMA) and PMMA are given in *Figure 22*. Of these materials, PMMA has the highest T_g and the lowest T_β. The T_g for the copolymer is below that for both homopolymers. Above the T_g, the α shift function can be described by the WLF equation with the constants given in *Table 2*. It is particularly difficult to ascertain the values of $\log a_T^\alpha$ at temperatures where the β transition occurs, and similar difficulties are incurred in obtaining the values of $\log a_T^\beta$ near the glass transition. The data indicate that the $\log a_T^\alpha$ function may become independent of temperature well below the glass transition as was observed by us before[10,11] for a series of epoxy resins; however, definitive limiting values could not be obtained. The two relaxation mechanisms clearly have different temperature dependences within their respective temperature regions.

The α mechanism relaxation spectra for PHEMA, P(HEMA-*co*-MMA) and PMMA are illustrated in *Figure 9*. The spectra shapes for all three polymers are essentially the same box-wedge shape that spans 11 to 13 decades of relaxation times. There is some evidence that PMMA has a second maximum at short relaxation times. These relaxation times correspond to data in the thermorheologically complex region between the α and β transition. This additional relaxation mechanism may

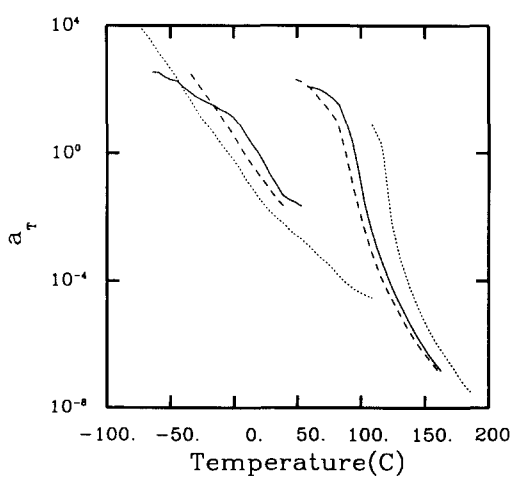

Figure 22 Independent shift functions a_T^β (left) and a_T^α (right) as a function of temperature for dry PHEMA (——), P(HEMA-*co*-MMA) (– –) and PMMA (-----)

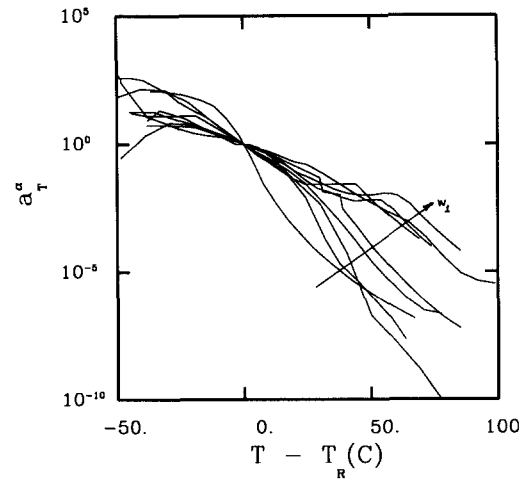

Figure 23 α-Mechanism shift functions for PHEMA hydrogels. Water weight fractions for the curves correspond in the direction of the arrow as follows: 0.000, 0.040, 0.049, 0.065, 0.085, 0.120, 0.200, 0.240 and 0.280

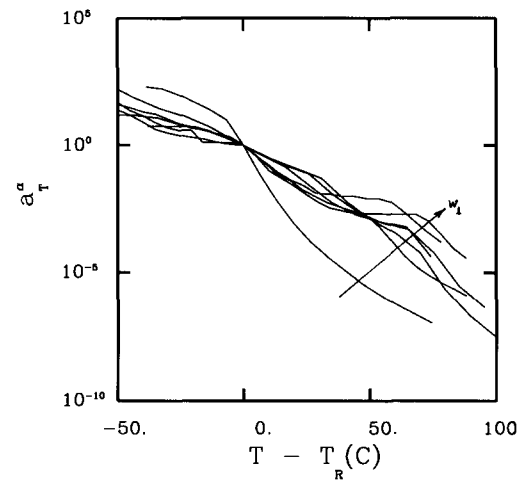

Figure 24 α-Mechanism shift functions for P(HEMA-*co*-MMA) hydrogels. Water weight fractions for the curves correspond in the direction of the arrow as follows: 0.000, 0.020, 0.040, 0.100, 0.110, 0.140 and 0.180

be an artifact from the α and β mechanisms not being completely resolved by the MMTTS analysis. Possible reasons for this will be presented in the Discussion section. The β mechanism relaxation spectra for PHEMA, P(HEMA-*co*-MMA) and PMMA polymers are given in *Figure 10*. Each spectrum is broadly distributed with a single maximum, which is more pronounced for the two polymers containing MMA repeat units.

Effect of water content

The α transition shift functions for the PHEMA and P(HEMA-*co*-MMA) hydrogels are given in *Figures 23* and *24*, respectively. The reference temperature for each curve has been selected as T_α at $1\,\mathrm{rad\,s^{-1}}$ for each composition as shown in *Figures 4* and *5*. The shift functions exhibit several notable characteristics. First of all, a linear change in temperature results in a logarithmic decrease in the shift function. Second, once the shift function is referred to the composition-dependent transition temperature, the temperature dependence of $\log a_T^\alpha$ deviates from that for the dry polymer curve and

Table 3 Empirical fit[a] of the PHEMA, P(HEMA-*co*-MMA) and PMMA data to shift functions

C (°C)	PHEMA	P(HEMA-*co*-MMA)	PMMA	T_R (°C)
α Transition at $w_1 = w_{1,eq}$	22.20±3.78	17.50±3.09	–	T_α at 1 rad s^{-1}
β Transition at $w_1 = 0$	15.66±0.55	16.90±0.62	17.68±0.64	T_β at 1 rad s^{-1}
β Transition at $w_1 = w_{1,eq}$	7.87±0.58	7.97±0.60	–	T_β at 1 rad s^{-1}

[a] Data fitted to the equation: $\log[a_T] = -\dfrac{T - T_R}{C}$

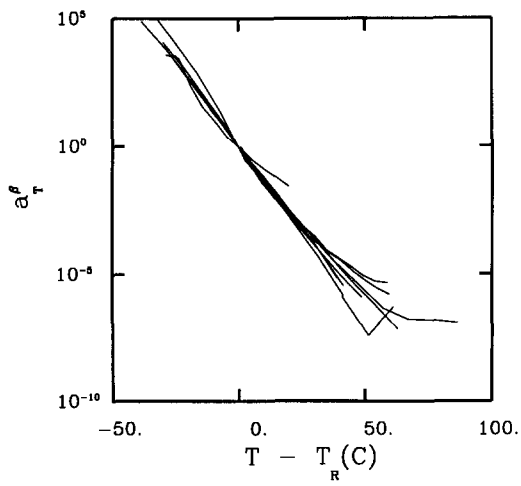

Figure 25 β-Mechanism shift functions for PHEMA hydrogels. Water weight fractions for the curves are 0.040, 0.049, 0.065, 0.085, 0.120, 0.160, 0.200 and 0.280. The curves are visually indistinguishable

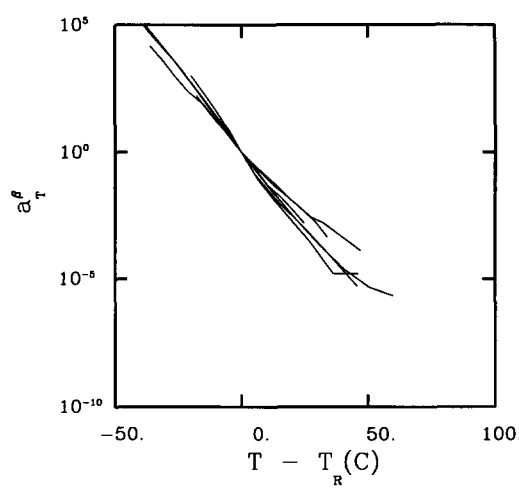

Figure 26 β-Mechanism shift functions for P(HEMA-*co*-MMA) hydrogels. Water weight fractions for the curves are 0.020, 0.040, 0.100, 0.140, 0.180 and 0.210. The curves are visually indistinguishable

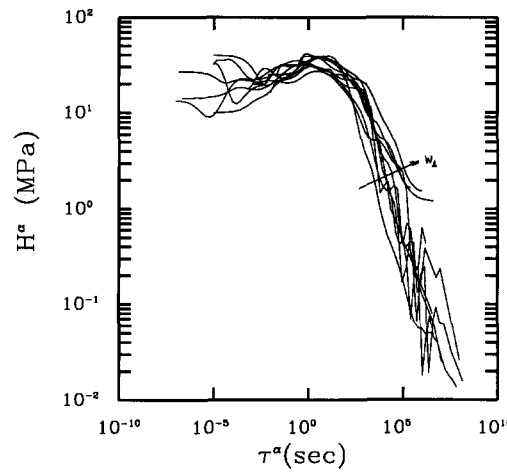

Figure 27 α-Mechanism viscoelastic spectra for PHEMA hydrogels. Water weight fractions for the curves correspond in the direction of the arrow as follows: 0.000, 0.040, 0.049, 0.065, 0.085, 0.120, 0.160, 0.200, 0.240 and 0.280

becomes quickly independent of composition. Deviations from the limiting curve at high temperatures can be readily attributed to water loss during the experimental measurements. *Table 3* presents the best-fitting semi-logarithmic correlation for the limiting curves at high water concentrations. The shift function at temperatures below the T_g is well known to depend on the thermal history of the sample. The result of ageing is to systematically lower the shift function in this temperature region[10]. The present study indicates there is a variation with composition in the shift function below the T_g. The shift function becomes systematically lower and more independent of temperature with increasingly higher water concentrations.

The β mechanism shift functions for the hydrogels are shown in *Figures 25* and *26*. It is quite unexpected that all $\log a_T^\beta$ data can be correlated linearly with temperature. Within the small scatter, the linear correlations are identical for both the PHEMA and copolymer hydrogels. There are some limited indications that $\log a_T^\beta$ becomes independent of temperature about 60°C above T_β, as seen in *Figure 25*. Here the α and β transitions for the PHEMA hydrogel ($w_1 = 0.21$) are better resolvable from the data.

The α mechanism viscoelastic spectra for the PHEMA and copolymer hydrogels are illustrated in *Figures 27* and *28*, respectively. Within experimental precision, these spectra are also essentially identical. There is a slight, systematic broadening to higher relaxation times with increasingly higher water concentrations most likely caused by a small loss of water during the measurement. The α relaxation mechanism does become increasingly better resolved with increased water concentrations as the spectral intensities begin to decrease at lower relaxation times. Still, the α spectra cannot be completely resolved at the lowest relaxation times due to the close proximity of the β transition for these isotherms.

The β mechanism spectra for PHEMA and copolymer hydrogels are illustrated in *Figures 29* and *30*, respectively. The widths and intensities of these spectra increase with higher water concentrations. The spectra for the PHEMA hydrogels deviate from that of the dry polymer rapidly with increased water concentration. The same, limiting spectrum intensity is attained from all PHEMA hydrogels studied. A more gradual, concentration

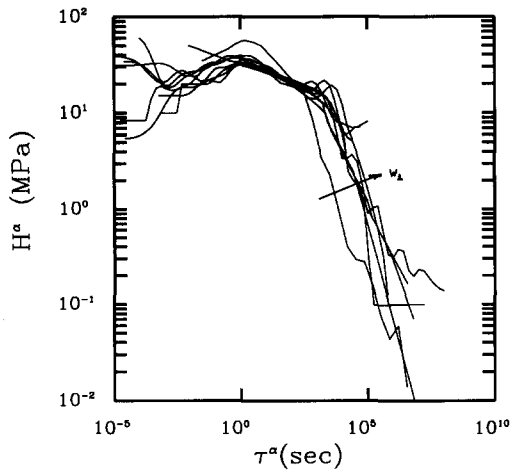

Figure 28 α-Mechanism viscoelastic spectra for P(HEMA-*co*-MMA) hydrogels. Water weight fractions for the curves correspond in the direction of the arrow as follows: 0.000, 0.020, 0.032, 0.040, 0.050, 0.100, 0.110, 0.140, 0.180 and 0.200

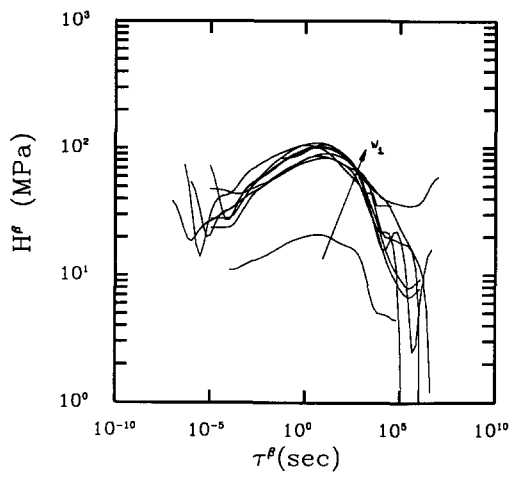

Figure 29 Discrete β-mechanism viscoelastic spectra for PHEMA hydrogels. Water weight fractions for the curves correspond in the direction of the arrow as follows: 0.000, 0.040, 0.065, 0.085, 0.120, 0.160, 0.200, 0.240 and 0.280

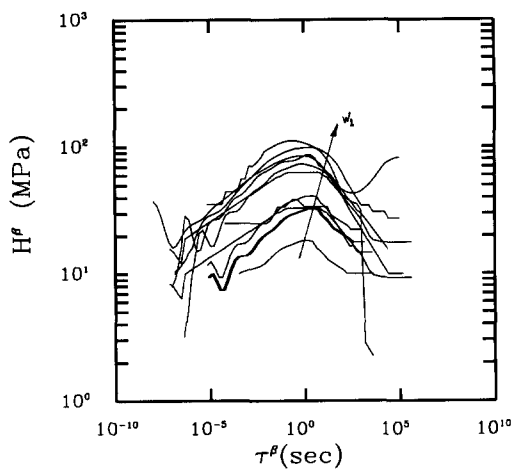

Figure 30 Discrete β-mechanism viscoelastic spectra for P(HEMA-*co*-MMA) hydrogels. Water weight fractions for the curves correspond in the direction of the arrow as follows: 0.000, 0.032, 0.049, 0.050, 0.061, 0.077, 0.090, 0.100, 0.110, 0.140, 0.180 and 0.200

dependent increase in the β spectra is observed for the copolymer hydrogels. Still, essentially the same, limiting spectral intensities are attained for both the PHEMA and copolymer hydrogels at high swelling. Some oscillations typically occur at the high and low relaxation time limits from the RQP algorithm due to there being only a truncated master curve available from the data. The master curve is limited at low relaxation times by the lowest attainable experimental temperature and at high relaxation times by the onset of the α transition.

The G_E values for the PHEMA and copolymer hydrogels are illustrated in *Figures 31* and *32*, respectively. Within experimental uncertainty, this calculated property is independent of shear rate. There is a decrease in this modulus of nearly three decades over the temperature region corresponding to the glassy–rubbery state transition. The calculated curves clearly possess both glassy and rubbery plateaus when data could be collected in the rubbery state. This indicates that these materials were effectively crosslinked. There are several trends exhibited with increasing water concentration: a

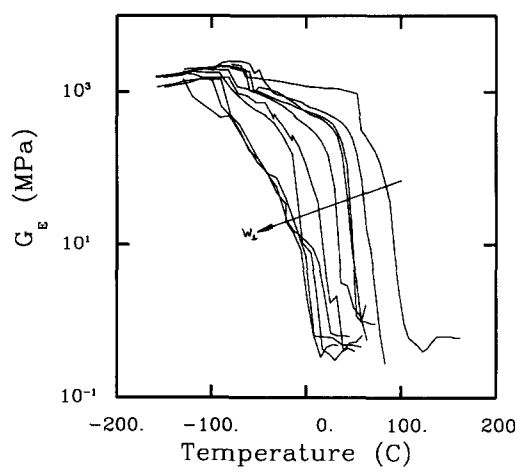

Figure 31 Temperature-dependent, elastic shear modulus, G_E, for PHEMA hydrogels. Water weight fractions for the curves correspond in the direction of the arrow as follows: 0.000, 0.040, 0.049, 0.065, 0.085, 0.120, 0.160, 0.200, 0.240 and 0.280

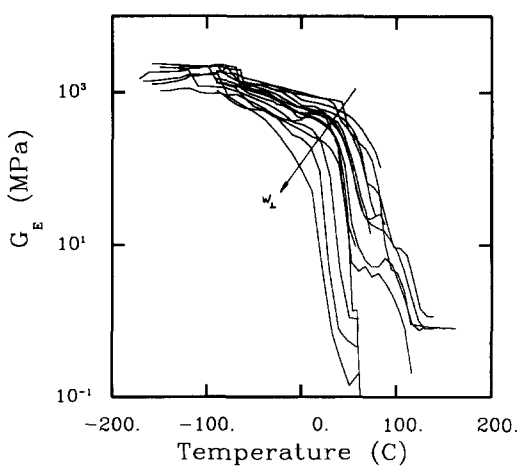

Figure 32 Temperature-dependent, elastic shear modulus, G_E, for P(HEMA-*co*-MMA) hydrogels. Water weight fractions for the curves correspond in the direction of the arrow as follows: 0.000, 0.020, 0.032, 0.040, 0.049, 0.050, 0.061, 0.077, 0.090, 0.100, 0.110, 0.140, 0.180 and 0.200

decrease in the value of the glassy plateau, a decrease in the apparent glassy–rubbery state transition temperature, and a decrease in the abruptness with which the transition occurs with increasing temperatures. The copolymer hydrogels show some evidence of water loss above 60°C by the presence of a small plateau artifact located just before the glassy–rubbery state transition temperature.

DISCUSSION

The viscoelastic behaviour of polymethacrylates considered in this investigation is only qualitatively similar to materials studied previously using a MMTTS analysis. For a series of poly(diglycidyl ether bisphenol-A-codiamino diphenylsulphone) epoxy resins[7], $T_\alpha - T_\beta$ is typically 200–300°C and the values of the loss modulus at the α and β transition peaks are typically 1–1.5 orders of magnitude larger than the average values between the two transitions. A MMTTS analysis on the epoxies results in well-resolved α and β relaxation spectra, notably at low values of the α mechanism relaxation times and high values of the β mechanism relaxation times. In contrast, the methacrylate materials studied in this investigation exhibit values of $T_\alpha - T_\beta$ on the order of 100°C or less. The maximum values of the loss modulus at the α and β transitions are typically less than twice the average glassy loss values between these transitions. In fact, the β transition is only a shoulder on the α transition for dry PHEMA in *Figure 1*. Hence the mechanical transitions in epoxies are much better separated and distinguishable over the experimentally attainable conditions.

This is somewhat surprising when one considers the molecular mechanisms attributed to the α and β relaxations of these polymers. For both the epoxy and methacrylate polymers, the α relaxation is generally attributed to large scale, cooperative displacements of the backbone chains in the macromolecular networks. The β relaxation in polymethacrylates is attributed to mechanically hindered pendant chain motions. In contrast, the β relaxation of the epoxies attributed to hindered crankshaft motions of hydroxyether and amine linkages, possibly correlated to phenylene ring flips[12]. Each of these groups are contained on the epoxy backbone chains and are not pendant groups. Between these two dissimilar polymers, it is interesting that the proximity to the backbone chain of the chemical groups believed to be responsible for β relaxations does not directly reflect the degree of correlation or separability between their respective α and β mechanical relaxations.

The MMTTS analysis provides a limited means to understand coupling between the α and β relaxation mechanisms. Were these two transitions completely uncoupled, we would expect the MMTTS analysis to provide two completely well-resolved sets of material functions for each transition because there is no explicit coupling scheme between mechanisms in the present MMTTS framework. The data in *Figures 1* and *2* vaguely suggest that these transitions might not be completely uncoupled since the loss modulus maxima at T_α and T_β are neither extremely prominent nor far apart in temperature. First of all, the long relaxation time portion of the β mechanism relaxation spectra appears to be correlated to the short relaxation time end of the α mechanism relaxation spectra since they do not completely resolve, i.e. they do not tail-off at these proximal ends. Second, isotherms used to construct these portions of the spectra correspond to a relatively narrow region of temperatures. The long relaxation time portion of the β spectra is computed mainly from isotherms at temperatures just higher than T_β. Likewise, the short relaxation time portion of the α spectra corresponds to isotherms at temperatures lower than T_α. Third, the apparent activation energy for the β mechanism shift function increases with increasing temperature and becomes comparable to the activation energy for the α mechanism shift function just below T_α. Consider an activation model for the β relaxation mechanism where we would expect the following Arrhenius expression to hold for the shift function.

$$a_T^\beta = \exp\left[\frac{E_a^\beta}{R}\left(\frac{1}{T} - \frac{1}{T_\beta}\right)\right] \tag{10}$$

However, an Arrhenius plot for the β mechanism shift functions illustrated in *Figures 25* and *26* does not yield a constant activation energy. In fact, the observed correlation implies the apparent activation energy is a decreasing function with increasing water content and an increasing function with increasing temperature.

$$E_a^\beta = \frac{2.303}{CT_\beta^{-1}} RT \tag{11}$$

The values of C and T_β are provided in *Table 3*. Similarly, the temperature dependence of the α mechanism shift function is not well described by equation (10) with a single activation energy. Hence, the molecular mechanisms responsible for these transitions cannot be described in terms of single, activated processes.

We might wish, however, to interpret our observed coupling between transitions in terms of the inferred molecular origins for these transitions as provided by previous studies[3–5]. Our data are reconcilable with these studies since the relative strengths of the β transitions for our samples are consistent with the relative contents of syndiotactic triads. The PHEMA has a smaller composition of syndiotactic triads than both the PMMA and copolymer samples; and, the magnitude of the β spectrum for PHEMA is commensurately weaker than those of PMMA and the copolymer. The less intense β relaxation has been attributed to be indicative of more hindered pendant chain rotational mobility. Now recall the β relaxation activation energy increases with temperature until the α transition predominates the relaxational response. Conceivably, increasingly larger segments would become involved with the β transition via correlated motions with increasing temperature. This would occur until several less hindered rotation elements exist concurrently along the polymer chains. At this point, the α mechanism becomes active and the glassy–rubbery transition occurs.

Water strongly affects the mechanical properties of both PHEMA and P(HEMA-*co*-MMA). There are two significant types of effects to consider: those related to the time- and frequency-dependent relaxation behaviour; and those related to the purely elastic, time- and frequency-independent behaviour. Most notably, the transition temperatures for the α, β and γ relaxations decrease significantly with increasing water content. The effect is most strongly pronounced for the decrease in the glassy– rubbery state transition temperature. With increasing water content, the α mechanism relaxation

spectra remain nearly invariant while there are significant, non-monotonic changes in the shift functions. In contrast, the β mechanism relaxation spectra significantly increased in intensity monotonically with increasing water content while the shift functions collapse to a single curve. The plasticization of these dynamic, viscoelastic properties is typically attributed to the water lending greater mobility to the macromolecules. This is consistent with the apparent activation energies for both the α and β mechanism shift factors decreasing with increasing water content. The fact that E_a^β decreases with increasing water content suggests that interchain mobility barriers are disrupted in the presence of water allowing increased pendant chain mobility. It is also observed that increasing water content has a marked effect on the frequency-independent shear modulus contribution, G_E, as illustrated in *Figures 31* and *32*. For each hydrogel composition, there are two clearly distinguishable drops in G_E as a function of temperature which occur consistently at the reference temperatures for the α and β mechanisms. Since this transition behaviour in G_E is both colligative and time-independent, it may reflect true transitions in the hydrogels' thermodynamic state. Although this MMTTS analysis is phenomenological, as far as we are aware, there does not currently exist a complete, fundamental framework in which to predict or describe these phenomena.

Fujita and Kishimoto[13] provided a phenomenological time–temperature–concentration superposition analysis for polymer–solvent systems. In their investigation, the isothermal Young's modulus was measured via stress relaxation after a known increase in solvent content from an incremental vapour sorption. For the systems studied: poly(vinyl acetate)–water, poly(vinyl acetate)–methanol, poly(methyl acrylate)–water and poly(methyl acrylate)–methanol, measurements could not be made at temperatures far below the glassy–rubbery state transition. However, the stress relaxation isotherms could be adequately superposed to a single master relaxation curve over a range of diluent concentrations and experimentally accessible temperatures and time duration. Moreover, the concentration-dependent shift factors were well described by the WLF equation. While the shift factors obtained from our data can also be fit by the WLF equation, this is true only for a narrow range of concentrations and temperatures. The limited applicability of the WLF equation is illustrated in *Figure 7*. As one lowers the temperature not too far below T_g, the WLF prediction for the shift factors diverges while the experimental shift factors actually level to a plateau. In addition, the WLF analysis does not address the existence of the β transition relaxation mechanism. Finally, we find that a relaxation spectrum and elastic modulus contribution are also required to reconstruct the entire linear viscoelastic response.

In conclusion, the PHEMA, P(HEMA-*co*-MMA) and PMMA materials exhibit thermorheologically complex behaviour at conditions far removed from the glassy–rubbery state transition, even in the absence of water. The data can be reasonably described by the sum of two distinct thermorheologically simple relaxation processes each with its own shift function. The dynamic response in the glassy–rubbery state transition is well described by the α relaxational mechanism alone and that for the first sub-T_g transition by the β relaxational mechanism. This approach supports the contention that relaxations at temperatures below T_g are not necessarily due entirely to glassy–rubbery state transition relaxation times frozen-in at low temperatures. Separate transition phenomena may exist at low temperatures. This approach is sufficiently general to study the effects of strongly plasticizing solvents.

ACKNOWLEDGEMENTS

This work was supported by a grant from the National Science Foundation to NAP. We wish to thank K. Bowles and F. Danko of the NASA Lewis Research Center and D. Curliss of the Wright-Patterson Air Force Base for the use of their dynamic mechanical spectrometers.

REFERENCES

1 Lustig, S. R., Caruthers, J. M. and Peppas, N. A. *Chem. Eng. Sci.* in press
2 Lustig, S. R. *PhD Thesis* Purdue University, 1989
3 Meier, D. J. 'Molecular Basis of Transitions and Relaxations', Gordon and Breach, New York, 1975
4 Russell, G. A., Hiltner, P. A., Gregonis, D. E., deVisser, A. C. and Andrade, J. D. *J. Polym. Sci., Polym. Phys. Edn* 1980, **18**,1271
5 Gillham, J. K. *AIChEJ.* 1974, **20**, 1066
6 Heijboer, J. *Int. J. Polym. Mater.* 1977, **6**, 11
7 Janaćek, J. *J. Macromol. Sci., Rev. Macromol. Chem.* 1973, **C9**, 1
8 Janaćek, J. and Kolarik, J. *Int. J. Polym. Mater.* 1976, **5**, 71
9 Ferry, J. D. 'Viscoelastic Properties of Polymers', 3rd Edn, Wiley, New York, 1980
10 Curliss, D. B. *MSChE Thesis* Purdue University, 1987
11 Curliss, D. B. and Caruthers, J. M. *Polym. Mater. Sci. Eng. Prepr.* 1987, **56**, 259
12 Takahama, T. and Geil, P. A. *J. Polym. Sci., Polym. Phys. Edn.* 1982, **20**, 1979
13 Fujita, H. and Kishimoto, A. *J. Polym. Sci.* 1958, **28**, 547